Physical Communication 8 (2013) 22–30

Contents lists available at ScienceDirect

Physical Communication

journal homepage: www.elsevier.com/locate/phycom

Full length article

Single-carrier frequency domain adaptive antenna array for uplink multi-user MIMO transmission in a cellular system

Wei Peng [a,b,*], Fumiyuki Adachi [b]

[a] *Huazhong University of Science and Technology, China*
[b] *Tohoku University, Japan*

ARTICLE INFO

Article history:
Received 30 October 2011
Accepted 13 February 2013
Available online 24 February 2013

Keywords:
Single-carrier
Multi-user MIMO
FDAAA
Link capacity

ABSTRACT

In this paper, single-carrier frequency domain adaptive antenna array (SC-FDAAA) for the uplink multi-user multiple-input multiple-output (MIMO) transmission in a cellular system is studied. By employing AAA weight control in frequency domain, the base station (BS) can suppress the multi-user interference (MUI) and therefore realize multi-user SC transmission. In addition, channel frequency selectivity can be exploited to obtain the frequency diversity (or the multi-path diversity). The frequency domain signal-to-interference-plus-noise-ratio (SINR) after weight control is investigated and the computational complexity of the proposed receiver is analyzed. In numerical simulations, cellular structure using the frequency reuse is assumed, and the effect of co-channel interference (CCI) is considered. The performance of the SC uplink multi-user MIMO transmission using SC-FDAAA is testified and compared with other multi-user detection schemes. The link capacity (maximum number of users/cell) and cellular link capacity (link capacity/frequency reuse factor) are also be evaluated.

© 2013 Elsevier B.V. All rights reserved.

1. Introduction

In the cellular system, the base station (BS) is usually equipped with multiple antennas and when multi-user transmission is considered, the multiple users together with the BS can be treated as a multiple-input multiple-output (MIMO) system [1]. In the uplink multi-user MIMO transmission, multiple antennas at the BS are usually used as MIMO multiplexing [2] or MIMO diversity [3]. In both cases, the degree of freedom is not used to suppress the interference. Another way to use the degree of freedom is to suppress the multi-user inference (MUI) by using adaptive antenna array techniques [4].

On the other hand, broadband transmission has been widely used in the wireless communication system. As a result of multi-path fading with large delay spread, the broadband wireless channel is severely frequency selectivity [5]. Therefore, it is necessary to suppress the inter-symbol interference (ISI). The ISI problem can be avoided by the use of multi-carrier transmission technique and the orthogonal frequency division multiple access (OFDMA) [6] has been adopted as a good solution for the downlink transmission. However, the multi-carrier transceivers are suffering from high peak to average power ratio (PAPR) problem which can lead to severe performance degradation. To avoid ISI as well as high PAPR problem, single-carrier frequency domain equalization (SC-FDE) has attracted much interest recently [7].

Furthermore, in the cellular system, the same carrier frequency is reused by spatially separated cells to increase the spectrum efficiency [8]. As a result, co-channel interference (CCI) becomes the dominant performance limitation instead of the thermal noise [9].

In our previous study [10], we proposed frequency domain adaptive antenna array (SC-FDAAA) to suppress MUI in the frequency selective fading channel. In this paper, we will study uplink multi-user MIMO transmission using SC-FDAAA. The signal-to-interference-plus-noise-ratio (SINR) as well as the computational complexity of SC-FDAAA receiver will be analyzed. In numerical simulations, the SC-FDAAA receiver will be compared with other multi-user

* Corresponding author at: Tohoku University, Japan.
E-mail address: peng@mobile.ecei.tohoku.ac.jp (W. Peng).

1874-4907/$ – see front matter © 2013 Elsevier B.V. All rights reserved.
http://dx.doi.org/10.1016/j.phycom.2013.02.001

detection algorithms and the link capacity will be evaluated as well.

The rest of the paper is organized as follows. The system model of SC uplink multi-user MIMO transmission in a cellular system is described in Section 2. The SC-FDAAA for MUI cancellation is described in Section 3. The frequency domain post SC-FDAAA SINR and the computation complexity analysis will be analyzed in Section 4. The performance of the SC-FDAAA will be compared with other multi-user detection algorithms and the link capacity given by the maximum number of users/cell will also be evaluated in Section 5. Finally this paper will be concluded in Section 6.

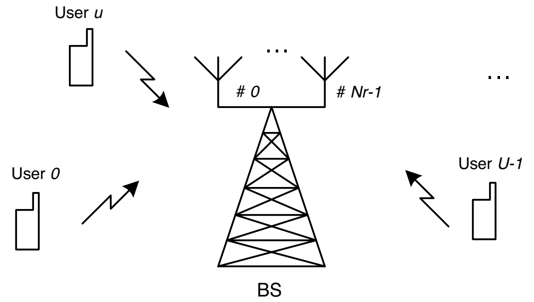

Fig. 1. Uplink transmission.

2. System model

We start from the simple case in a single cell. The system model of SC uplink multi-user MIMO transmission is shown in Fig. 1. It is assumed that, the BS is equipped with N_r receive antennas. The number of active users per cell is U and each user has one transmit antenna. Therefore, the uplink transmission between the U users and the BS is carried out in a $U \times N_r$ MIMO channel. A block fading channel between each user and the BS is assumed, i.e., the channel remains unchanged during the transmission period of a block. In this paper, the symbol-spaced discrete time representation of the signal is used. Assuming an L-path channel, the impulse response of the channel between user u and the mth antenna of the BS can be expressed as

$$h_{u,m}(\tau) = \sum_{l=0}^{L-1} h_{u,m,l}\delta(\tau - \tau_l), \tag{1}$$

where $h_{u,m,l}$ and τ_l are the path gain and time delay of the lth path, respectively. $h_{u,m,l}$ follows the complex Gaussian distribution (Rayleigh distribution) and satisfies $\sum_{l=0}^{L-1} E\{|h_{u,m,l}|^2\} = 1$ where $E\{\cdot\}$ represents the expectation operation. It is assumed that, the time delay τ_l is a multiple integer of the symbol duration and $\tau_l = l$. The cyclic-prefixed block signal transmission is used to avoid inter block interference (IBI) and it is assumed that, the cyclic prefix (CP) is longer than the maximum path delay of the signal. In the following, we omit the insertion and removal of the CP for the purpose of simplicity.

The baseband equivalent received signal block $\{r_m(t);\ t = 0 \sim N_c - 1\}$ of N_c symbols at the mth antenna is given by

$$r_m(t) = \sum_{u=0}^{U-1} \sqrt{P_u d_u^{-\alpha} 10^{-\xi_u/10}} \sum_{l=0}^{L-1} h_{u,m,l} s_u(t-l) + n_m(t), \tag{2}$$

where $s_u(t)$ and P_u are the transmit signal and transmit signal power of user u ($u = 0 \sim U - 1$), respectively. d_u represents the distance between user u and the BS; α and ξ represent the path loss exponent and shadowing loss in dB, respectively. To simplify the analysis, $\xi = 0$ (no shadowing loss) is assumed. $n_m(t)$ is the additive white Gaussian noise (AWGN).

According to (2), the frequency domain representation of the received signal at the mth antenna on the kth frequency is given by [11]

$$R_m(k) = \sum_{u=0}^{U-1} H_{u,m}(k) S_u(k) + N_m(k), \tag{3}$$

where

$$\begin{cases} S_u(k) = \sqrt{P_u} \sum_{t=0}^{N_c-1} s_u(t) \exp\left(-j2\pi k \frac{t}{N_c}\right) \\ H_{u,m}(k) = \sum_{l=0}^{L-1} \sum_{t=0}^{N_c-1} h_{u,m,l} \exp\left(-j2\pi k \frac{t}{N_c}\right) \\ N_m(k) = \sum_{t=0}^{N_c-1} n_m(t) \exp\left(-j2\pi k \frac{t}{N_c}\right). \end{cases} \tag{4}$$

The frequency domain received signal vector on the kth frequency $\mathbf{R}(k)$ is then expressed as

$$\mathbf{R}(k) = \sum_{u=0}^{U-1} \mathbf{H}_u(k) S_u(k) + \mathbf{N}(k), \tag{5}$$

where $\mathbf{H}_u(k) = \left[H_{u,0}(k) \quad H_{u,1}(k) \quad \cdots \quad H_{u,N_r-1}(k)\right]^T$ and $\mathbf{N}(k) = \left[N_0(k) \quad N_1(k) \quad \cdots \quad N_{N_r-1}(k)\right]^T$ with the superscript ^{T} representing transpose operation.

In the cellular environment, there exists CCI from the neighboring co-channel cells due to the frequency reuse. The frequency reuse in cellular systems is shown in Fig. 2, where the frequency reuse factors (FRF) are 1, 3, 4 and 7, respectively. The commonly used first layer CCI model [9] is used here, i.e., only the CCI from the first layer neighboring co-channel cells will be considered and the number of CCI cells will be $B = 6$. The received signal in (2) should be modified to include the CCI, and it can be rewritten as

$$\begin{aligned} r_m(t) = {} & \sum_{u=0}^{U-1} \sqrt{P_u d_u^{-\alpha}} \sum_{l=0}^{L-1} h_{u,m,l} s_u(t-l) \\ & + \sum_{i=1}^{B} \sum_{u_i=0}^{U_i-1} \sqrt{P_{i,u_i} d_{i,u_i}^{-\alpha}} \sum_{l=0}^{L-1} c_{i,u_i,m,l} s_{i,u_i}(t-l) \\ & + n_m(t), \end{aligned} \tag{6}$$

where s_{i,u_i} and P_{i,u_i} are respectively the transmit signal and transmit signal power of the u_ith user in the ith co-channel cell; d_{i,u_i} and $c_{i,u_i,m,l}$ are the distance and channel gain between the CCI user and the BS, respectively.

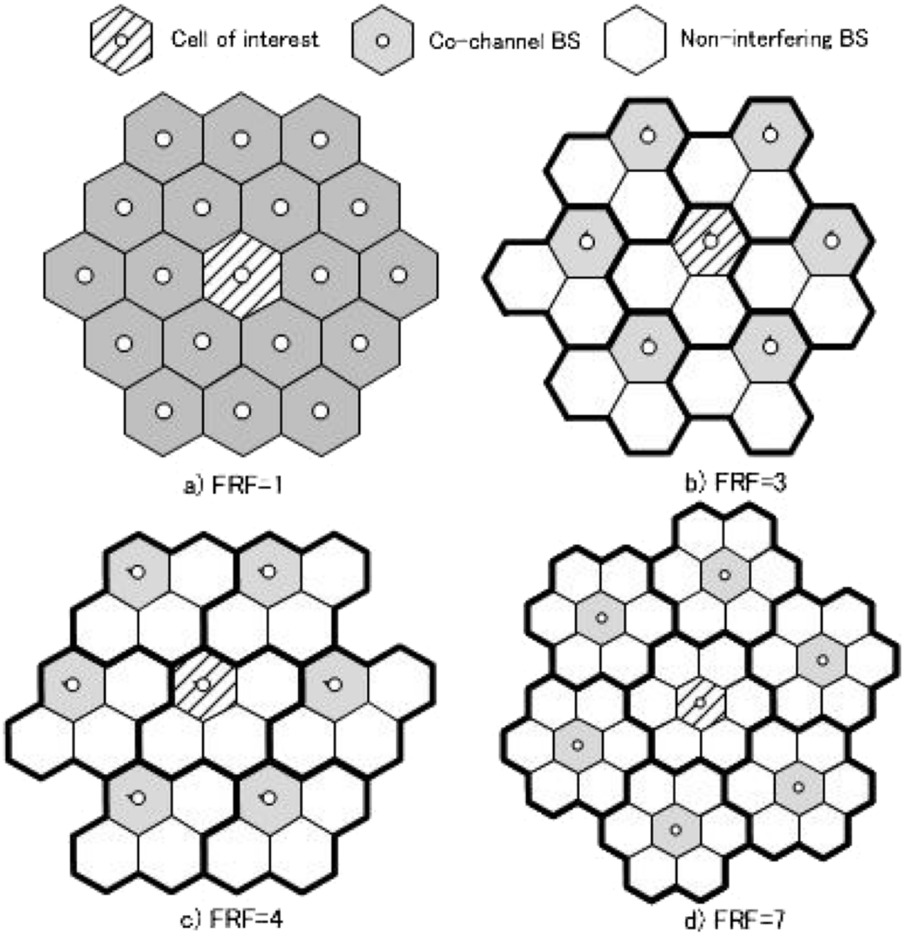

Fig. 2. Frequency reuse in cellular systems.

The frequency domain received signal on the kth frequency for (6) is given by

$$R_m(k) = \sum_{u=0}^{U-1} H_{u,m}(k)S_u(k) + \sum_{i=1}^{B}\sum_{u_i=0}^{U_i-1} C_{i,u_i,m}(k)S_{i,u_i}(k) + N_m(k), \quad (7)$$

where

$$\begin{cases} S_{i,u_i}(k) = \sqrt{P_{i,u_i}d_{i,u_i}^{-\alpha}} \sum_{t=0}^{N_c-1} s_{i,u_i}(t) \exp\left(-j2\pi k \dfrac{t}{N_c}\right) \\ C_{i,u_i,m}(k) = \sum_{l=0}^{L-1}\sum_{t=0}^{N_c-1} c_{i,u_i,m,l} \exp\left(-j2\pi k \dfrac{t}{N_c}\right) \end{cases} \quad (8)$$

and the second term in the right-hand-side of (7) is the CCI component.

In our study, slow transmit power control (TPC) in each cell is assumed and the transmit power of each user in each cell is controlled, so that the average signal-to-noise ratio (SNR) received at the corresponding BS is kept at the target SNR, i.e.

$$\begin{cases} P_u/\sigma^2 = \Gamma_{\text{TPC\_Target}}\, d_i^{\alpha} \\ P_{i,u_i}/\sigma^2 = \Gamma_{\text{TPC\_Target}}\, d_{i,u}^{\alpha}, \end{cases} \quad (9)$$

where $\Gamma_{\text{TPC\_Target}}$ is the TPC target SNR and σ^2 is the noise power.

3. SC-FDAAA algorithm

3.1. Transmitter

The transmitter structure is illustrated in Fig. 3(a) [12]. Binary data sequence is modulated and divided into a sequence of blocks of N_c data symbols. The last N_g symbols in each block are copied and inserted as the cyclic prefix into the guard interval (GI) and placed at the beginning of each block. In addition, pilot signals will be transmitted for channel estimation and AAA weight control. The frame structure of the transmit signal is shown in Fig. 3(b).

3.2. Receiver structure

The transmit signals from the U users will be recovered from (7) one by one at the BS by using AAA weight control.

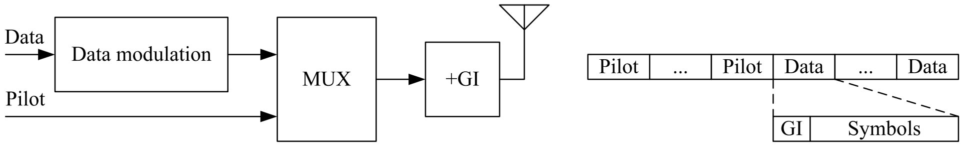

(a) Transmitter structure.

(b) Transmit frame structure.

Fig. 3. Transmitter structure and transmit frame structure.

The structure of SC-FDAAA receiver is shown in Fig. 4. AAA weight control is applied on each frequency. Given the frequency domain received signal in (7), AAA weight control is performed as

$$\tilde{R}(k) = \mathbf{W}_{\text{FDAAA}}^{T}(k)\mathbf{R}(k), \tag{10}$$

where $\mathbf{W}_{\text{FDAAA}}(k) = [W_{\text{FDAAA},0}(k), \ldots, W_{\text{FDAAA},N_r-1}(k)]^T$ is the SC-FDAAA weight control vector. The SC-FDAAA weight is designed to minimize the mean squared error (MSE) between the SC-FDAAA output and the reference signal (in this study the pilot sequence is used as the reference signal). Take the transmit signal from the 0th user as an example. The MSE is given by

$$\begin{aligned} &E\{E^2(k)\} \\ &= E\{[S_0(k) - \mathbf{W}_{\text{FDAAA}}^{T}(k)\mathbf{R}(k)]^*[S_0(k) \\ &\quad - \mathbf{W}_{\text{FDAAA}}^{T}(k)\mathbf{R}(k)]\} \\ &= E\left\{ \begin{array}{c} S_0^*(k)S_0(k) - S_0^*(k)\mathbf{W}_{\text{FDAAA}}^{T}(k)\mathbf{R}(k) \\ -\mathbf{R}^*(k)\mathbf{W}_{\text{FDAAA}}^{H}(k)S_0(k) \\ +\mathbf{R}^*(k)\mathbf{W}_{\text{FDAAA}}^{H}(k)\mathbf{W}_{\text{FDAAA}}^{T}(k)\mathbf{R}(k) \end{array} \right\}, \end{aligned} \tag{11}$$

where $E\{\cdot\}$ denotes the ensemble operation, superscript * represents the conjugate and superscript H represents the conjugate transpose operation. To minimize the MSE in (11), the SC-FDAAA weight $\mathbf{W}_{\text{FDAAA}}(k)$ must satisfy the following equality

$$\frac{\partial E\{E^2(k)\}}{\partial \mathbf{W}_{\text{FDAAA}}(k)} = 0. \tag{12}$$

By substituting (11) into (12), the following equality is obtained

$$E\{-2S_0(k)\mathbf{R}^*(k) + 2\mathbf{R}^*(k)\mathbf{R}(k)\mathbf{W}_{\text{FDAAA}}(k)\} = 0. \tag{13}$$

By solving (13), the SC-FDAAA weight vector $\mathbf{W}_{\text{FDAAA}}(k)$ is obtained as [13]

$$\mathbf{W}_{\text{FDAAA}}(k) = \mathbf{C}_{rr}^{-1}(k)\mathbf{C}_{rd}(k), \tag{14}$$

where

$$\begin{aligned} \mathbf{C}_{rr}(k) &= E\{\mathbf{R}^*(k)\mathbf{R}(k)\} \\ &= \mathbf{A}_0^*(k)\mathbf{A}_0(k) + \sum_{u=1}^{U-1}\mathbf{A}_u^*(k)\mathbf{A}_u(k) \\ &\quad + \sum_{i=1}^{B}\sum_{u_i=0}^{U_i-1}\mathbf{A}_{i,u_i}^*(k)\mathbf{A}_{i,u_i}(k) + N_0\mathbf{I} \\ &= \mathbf{A}_0^*(k)\mathbf{A}_0(k) + \mathbf{N}'(k), \end{aligned} \tag{15}$$

and

$$\mathbf{C}_{rd}(k) = E\{\mathbf{R}^*(k)S_0(k)\} = \mathbf{A}_0(k)S_0(k). \tag{16}$$

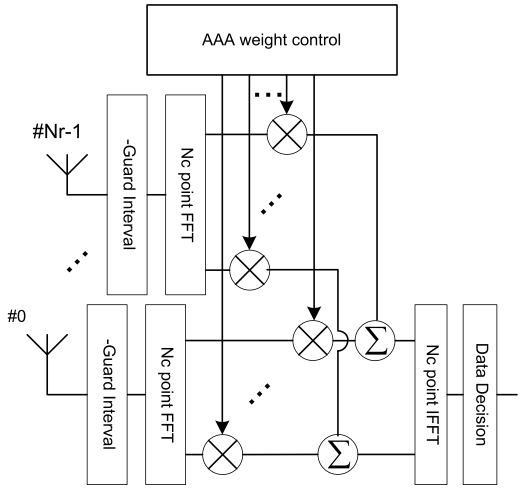

Fig. 4. Structure of FDAAA receiver.

In (15), $\mathbf{A}_0(k) = \mathbf{H}_0(k)S_0(k)$ represents the propagation vector [14] of the transmit signal from the desired user, $\mathbf{A}_i(k)$ and $\mathbf{A}_{i,u_i}(k)$ are the propagation vectors of the transmit signal from the MUI and CCI, respectively. It is assumed that, the inference signals, the desired signal and the noise signal are uncorrelated with each other. N_0 represents the power spectrum density of the AWGN (which is white in frequency domain) and $\mathbf{I}$ is an $N_r \times N_r$ standard matrix. $\mathbf{N}'(k)$ is used to represent the interference plus noise.

After performing the SC-FDAAA weight control, the time domain signal block estimate is obtained by N_c-point IFFT as

$$\hat{d}(t) = \frac{1}{N_c}\sum_{k=0}^{N_c-1}\hat{R}(k)\exp\left(-j2\pi k\frac{t}{N_c}\right) \tag{17}$$

for data decision.

4. SINR analysis and computational complexity analysis

The SINR after the weight control on the kth frequency can be evaluated by [13]

$$\Gamma(k) = \frac{\mathbf{W}_{\text{FDAAA}}^{H}(k)\mathbf{R}_s(k)\mathbf{W}_{\text{FDAAA}}^{(k)}}{\mathbf{W}_{\text{FDAAA}}^{H}(k)\mathbf{R}_{NI}(k)\mathbf{W}_{\text{FDAAA}}^{(k)}}, \tag{18}$$

where $\mathbf{R}_s(k)$ and $\mathbf{R}_{NI}(k)$ are the auto-correlation matrix of the received desired signal and the interference plus noise, respectively.

Property. *If a matrix* $\mathbf{Z}$ *can be written as* $\mathbf{Z} = \mathbf{T}^{-1} + \mathbf{P}\mathbf{Q}^{-1}\mathbf{P}^*$, *then the inverse matrix of* $\mathbf{Z}$ *can be obtained by* [15,16]

$$\mathbf{Z}^{-1} = \mathbf{T} - \mathbf{T}\mathbf{P}(\mathbf{Q} + \mathbf{P}^*\mathbf{T}\mathbf{P})^{-1}\mathbf{P}^*\mathbf{T}. \tag{19}$$

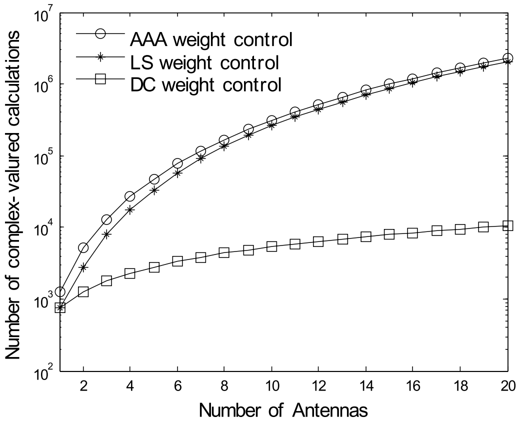

Fig. 5. Computational complexity comparison.

Let $\mathbf{Z} = \mathbf{C}_{rr}(k)$, $\mathbf{T} = \mathbf{R}_{NI}^{-1}(k)$, $\mathbf{P} = \mathbf{A}_0^*(k)$ and $\mathbf{Q} = \mathbf{I}$, then the inverse matrix $\mathbf{C}_{rr}^{-1}(k)$ can be calculated by submitting $\mathbf{Z}$, $\mathbf{T}$, $\mathbf{P}$ and $\mathbf{I}$ into (19)

$$\begin{aligned}\mathbf{C}_{rr}^{-1} &= \mathbf{R}_{NI}^{-1}(k) - \mathbf{R}_{NI}^{-1}(k)\mathbf{A}_0^*(k)[\mathbf{I} + \mathbf{A}_0(k)\mathbf{R}_{NI}^{-1}\mathbf{A}_0^*(k)]^{-1} \\ &\quad \times \mathbf{A}_0(k)\mathbf{R}_{NI}^{-1}(k) \\ &= \mathbf{R}_{NI}^{-1}(k)\left[\mathbf{I} - \frac{\mathbf{A}_0^*(k)\mathbf{A}_0(k)\mathbf{R}_{NI}^{-1}(k)}{\mathbf{I} + \mathbf{A}_0(k)\mathbf{R}_{NI}^{-1}\mathbf{A}_0^*(k)}\right] \\ &= \left[\frac{1}{1 + \mathbf{A}_0(k)\mathbf{R}_{NI}^{-1}\mathbf{A}_0^*(k)}\right]\mathbf{R}_{NI}^{-1}(k).\end{aligned} \tag{20}$$

The SC-FDAAA weight is then obtained by substituting (16) and (20) into (14), given by

$$\begin{aligned}\mathbf{W}_{\text{FDAAA}}(k) &= \left[\frac{1}{1 + \mathbf{A}_0(k)\mathbf{R}_{NI}^{-1}\mathbf{A}_0^*(k)}\right] \\ &\quad \times \mathbf{R}_{NI}^{-1}(k)\mathbf{A}_0(k)S_0(k).\end{aligned} \tag{21}$$

Finally, the SINR after the weight control can be expressed, by substituting (21) into (18), as

$$\Gamma(k) = \mathbf{A}_0(k)\mathbf{R}_{NI}^{-1}(k)\mathbf{A}_0^*(k). \tag{22}$$

In the next, we discuss the computational complexity of the proposed SC-FDAAA receiver for uplink multi-user MIMO transmission in terms of the number of complex-valued multiplication operations. Since FFT and IFFT calculations have fixed computational complexity, here we focus on the frequency domain signal processing. From the Eqs. (10) and (14)–(16), the computational complexity for each frequency is composed by the calculation of $\mathbf{C}_{rr}$, $\mathbf{C}_{rd}$, $\mathbf{C}_{rr}^{-1}$, $\mathbf{C}_{rr}^{-1}\mathbf{C}_{rd}$ and $\mathbf{W}_{\text{FDAAA}}^T(k)\mathbf{R}(k)$. The computational complexity of each part in the frequency domain signal processing is listed in Table 1. In order to make comparison, the computation complexity of diversity combing (DC) and least square (LS) schemes (the details of these two schemes will be described in Section 5) is also listed. Note that, channel estimation is necessary and the simple least square channel estimation is assumed which costs one complex-valued multiply operation on each frequency.

Given $N_c = 256$, the numbers of complex-valued multiplications are shown in Fig. 5 as an example. It is shown that, DC algorithm has the lowest complexity among the three algorithms. On the other hands, FDAAA algorithm and LS algorithm have similar complexity, especially when the number of antennas increases.

5. Simulation results

In this section, the performance of the uplink multi-user MIMO transmission using SC-FDAAA will be investigated. To focus on the proposed algorithm itself, no channel coding is used. In addition, $\xi = 0$ (no shadowing loss) is assumed as already mentioned in Section 2. The parameters used in the simulations are listed in Table 2.

5.1. Bit error rate performance (BER)

The BER performance of the SC-FDAAA for uplink multi-user MIMO transmission is compared with two other detection schemes at first. The reference schemes are DC and a LS schemes. All the three detection schemes use the same transmitter structure. In DC scheme, MUI is treated as noise, so that diversity combining techniques can be used. The signal after DC on the kth frequency is expressed by

$$\tilde{R}_{\text{FDDC}}(k) = \mathbf{W}_{\text{FDDC}}^T(k)\mathbf{R}(k), \tag{23}$$

where $\mathbf{W}_{\text{FDDC}}(k) = [W_{\text{FDDC},0}(k), \ldots, W_{\text{FDDC},N_r-1}(k)]^T$ is the DC weight. The DC weight is given for various diversity combining criteria as [17].

$$\mathbf{W}_{\text{FDDC}}(k) = \begin{cases} \dfrac{[H_{0,0}^*(k), \ldots, H_{0,N_r-1}^*(k)]^T}{\sum_{m=0}^{N_r-1}|H_{0,m}(k)|^2} & \text{ZF} \\ \left[\dfrac{H_{0,0}^*(k)}{|H_{0,0}^*(k)|}, \ldots, \dfrac{H_{0,N_r-1}^*(k)}{|H_{0,N_r-1}^*(k)|}\right]^T & \text{EGC} \\ \left[H_{0,0}^*(k), \ldots, H_{0,N_r-1}^*(k)\right]^T & \text{MRC} \\ \dfrac{\left[H_{0,0}^*(k), \ldots, H_{0,N_r-1}^*(k)\right]^T}{\sum_{m=0}^{N_r-1}|H_{0,m}(k)|^2 + (\sigma^2 + P_I)/P_0} & \text{MMSE} \end{cases} \tag{24}$$

where ZF, EGC, MRC and MMSE represent the corresponding DC techniques, P_I is the interference power. It is shown in [17] that, when $N_r \geq 2$, ZF DC and MMSE DC have almost the same BER performance. Therefore, ZF DC will be used for its simplicity.

For LS scheme, the signal estimate on the kth frequency is given by [2]

$$\hat{R}_{\text{LS}}(k) = \mathbf{H}^H(k)\left(\mathbf{H}(k)\mathbf{H}^H(k)\right)^{-1}\mathbf{R}(k), \tag{25}$$

where $\mathbf{H}(k) = \left[\mathbf{H}_0(k) \quad \cdots \quad \mathbf{H}_{U-1}(k)\right]$.

BER performance comparison between the three detection schemes are made by assuming four receive antennas ($N_r = 4$) and the number of users varies from $\{1, \ldots, N_r\}$ ($U = 1, \ldots, 4$), the results are shown in Fig. 6. At first, $U = 1$ is used so that no MUI exists. The BER performance is shown in Fig. 6(a). It is observed that, the three schemes have almost the same performance when no MUI exists. In

Table 1
Computational complexity.

Detection algorithm	Number of complex-valued multiplications on each frequency		Total computational complexity
SC-FDAAA	Channel estimation	1	$N_c O(N_r^3 + 2N_r^2 + 2N_r + 1)$
	$\mathbf{C}_{rr}$	$O(N_r^2)$	
	$\mathbf{C}_{rd}$	$O(N_r)$	
	$\mathbf{C}_{rr}^{-1}$	$O(N_r^3)$	
	$\mathbf{C}_{rr}^{-1}\mathbf{C}_{rd}$	$O(N_r^2)$	
	$\mathbf{W}_{\text{FDAAA}}^T(k)\mathbf{R}(k)$	$O(N_r)$	
MIMO multiplexing Least square algorithm	Channel estimation	1	$N_c O(N_r^3 + N_r + 1)$
	$\mathbf{H}^H(k)(\mathbf{H}(k)\mathbf{H}^H(k))$	$O(N_r^3)$	
	$\mathbf{H}^H(k)(\mathbf{H}(k)\mathbf{H}^H(k))\mathbf{R}(k)$	$O(N_r)$	
MIMO diversity Diversity combining algorithm	Channel estimation	1	$N_c O(2N_r + 1)$
	$\frac{\left[H_{0,0}^*(k),\ldots,H_{0,N_r-1}^*(k)\right]^T}{\sum_{m=0}^{N_r-1} \lvert H_{0,m}(k)\rvert^2}$	$O(N_r)$	
	$\mathbf{W}_{\text{FDDC}}^T(k)\mathbf{R}(k)$	$O(N_r)$	

Table 2
Simulation parameters.

Modulation		QPSK
TPC target SNR $\Gamma_{\text{TPC\_Target}}$		$\to \infty$
Frequency reuse factor (FRF)		1,3,4,7
Channel	Channel model	Frequency selective block Rayleigh fading
	Path loss exponent α	2.5 3.5
	Number of paths L	16
	Power delay profile	Uniform
Number of antennas N_r		2–8
Number of users U in each cell		$1 \sim N_r$
Receiver algorithms		SC-FDAAA (proposed) DC LS
Locations of users		Randomly distributed
FFT block size N_c		256

the next, the number of users U increases from 2 to 4, and the BER performances of the three schemes are shown in Fig. 6(b)–(d), respectively. Our finding is four-fold. Firstly, the performance of the three algorithms all degrades when the number of users increases. This result is implied by the SINR expression in (22). When the number of receive antennas is fixed, the prorogation vector $\mathbf{A}_0(k)$ in (22) will be fixed as well. When the number of users in each cell increases, the number of MUI will increase, and the CCI power will also increase. Therefore, the components of the auto-correlation matrix $\mathbf{R}_{NI}(k)$ of interference plus noise in (22) will also increase in their values. As a result, the post SC-FDAAA SINR will decrease and then BER performance will degrade; Secondly, the performance of SC-DC scheme suffers from significant error floor when $U \geq 2$. The reason is that, as already mentioned, the MUI is treated as noise in SC-DC scheme. When $U \geq 2$, MUI will dominate the BER performance instead of the noise. Therefore, significant error floor occurs in the BER curves of SC-DC scheme; Thirdly, SC-FDAAA scheme achieves better performance than that of SC-LS scheme. This is because that, the objective of SC-FDAAA scheme is to minimize the square error between the signal estimate and the transmitted signal of the desired user, while the objective of the SC-LS scheme is to minimize the square error of the signal estimate vector and the transmitted signal vector. As a result, the SC-LS scheme will increase the noise power on the desired user while the SC-FDAAA scheme will not. Therefore, the SC-FDAAA can achieve better performance than the LS scheme; Finally, SC-DC algorithm achieves the best performance in low SNR region in the case when $U = 4$. The reason is that, when $U = 4$, all the degree of freedom of the receive antennas will be used to suppress the MUI for SC-FDAAA scheme, as well as the LS scheme. Since the performance of SC-FDAAA and SC-LS scheme are dominated by noise, the diversity gain achieved by the SC-DC scheme can yield better performance in low SNR region.

The BER performance of the uplink SC multi-user MIMO transmission as a function of active users and FRF is studied in the next. In this simulation, $N_r = 8$ is used and the number of users in each cell varies from 1 to 8. We compared the BER performance when the path loss exponent α varies between 2.5 and 3.5, and the results are shown in Figs. 7 and 8, respectively. It is assumed that, the target SNR $\Gamma_{\text{TPC\_Target}}$ approximates infinite. As a result, the BER is determined by the MUI and CCI only. It is observed from both Figs. 7 and 8 that, the BER performance can be improved when a larger FRF is used. The reason is that, when the FRF increases, the distance between the CCI user and the BS will increase. Given a fixed path loss exponent, the CCI power will be reduced and the BER performance will be improved.

By comparing the results in Fig. 7 when $\alpha = 2.5$ and the results in Fig. 8 when $\alpha = 3.5$, it is observed that, when a larger path loss exponent is used, a better BER performance can be achieved when the other parameters remain the

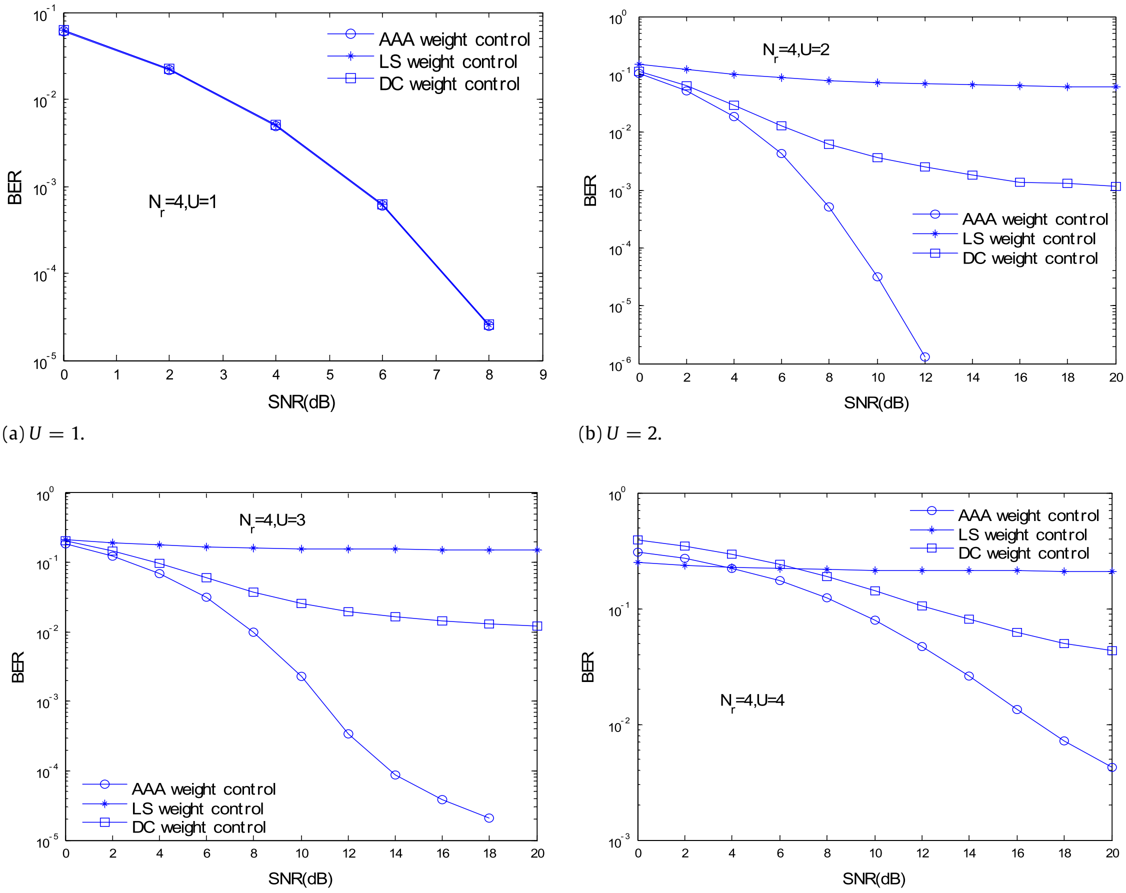

(a) $U = 1$.

(b) $U = 2$.

(c) $U = 3$.

(d) $U = 4$.

Fig. 6. BER performance comparison.

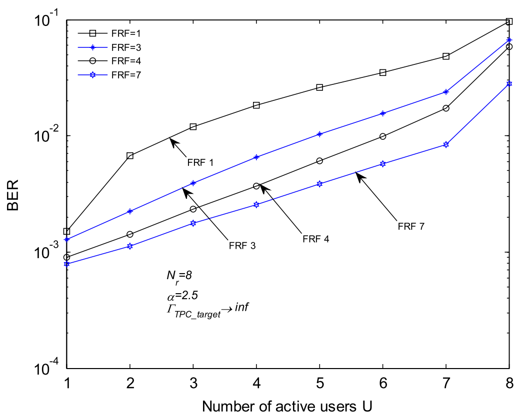

Fig. 7. BER performance of uplink SC multi-user MIMO detection, $\alpha = 2.5$.

same. The reason of the BER performance improvement is that, when a larger path loss exponent is used, the signal power of CCI user will reduce if the location of the CCI user remains unchanged. On the other hand, the signal power of MUI remains the same because the TPC control guarantees the same SNR target of different users. As a result, the post SC-FDAAA SINR decreases and the BER performance improves.

5.2. Link capacity and cellular link capacity

Next, we invested the link capacity given by the maximum number of users/cell. Since we are considering uncoded system, the target BER is set to be 10^{-3} with an outage rate of 10% ($Q = 0.1$). The maximum number of users/cell as a function of receive antennas using $\alpha = 2.5$ and $\alpha = 3.5$ are shown in Figs. 9 and 10, respectively. It is observed that, by using the SC-FDAAA to suppress the MUI, SC uplink cellular multi-user MIMO transmission can be realized. When $\alpha = 2.5$, the multi-user MIMO transmission can be realized only when FRF > 1; For example, when the BS has 8 antennas, each cell can accommodate a maximum number of 4 users when FRF $= 7$. When $\alpha = 3.5$, uplink cellular multi-user MIMO transmission can be realized for all the FRFs including FRF $= 1$. Two users/cell can be accommodated by a BS with 8 antennas when FRF $= 1$. And 5 users/cell can be accommodated by a BS with 7 antennas when FRF $= 7$ is used.

By using a larger FRF, more bandwidth will be used in cellular system. Therefore, the cellular link capacity defined as link capacity normalized by FRF factor is also an

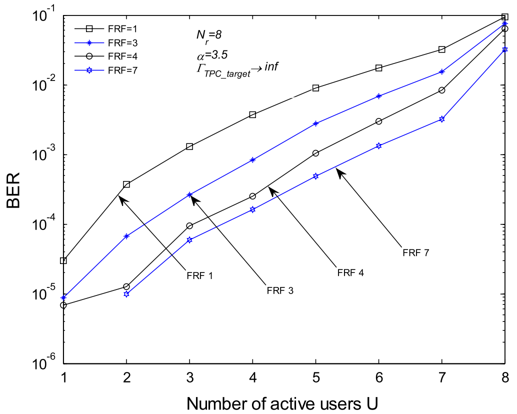

Fig. 8. BER performance of uplink SC multi-user MIMO detection, $\alpha = 3.5$.

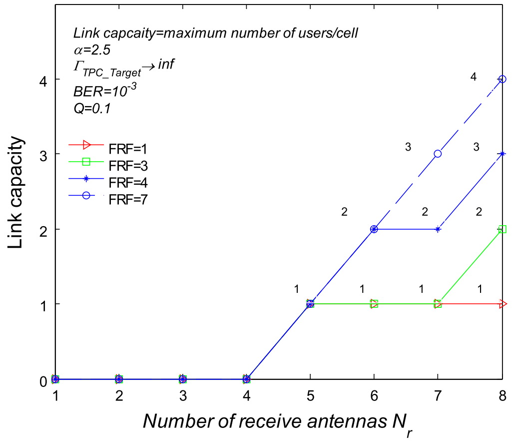

Fig. 9. Link capacity, $\alpha = 2.5$.

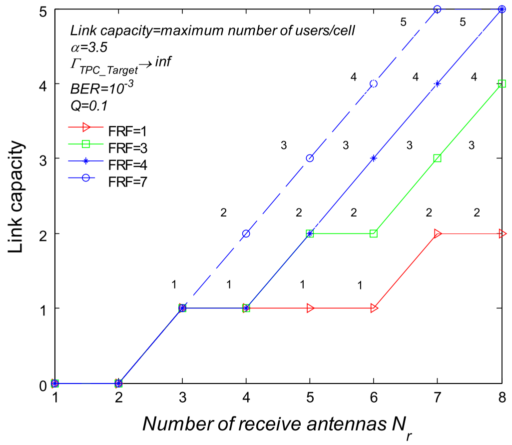

Fig. 10. Link capacity, $\alpha = 3.5$.

important capacity evaluation. The cellular link capacity is then shown in Figs. 11 and 12 for $\alpha = 2.5$ and $\alpha = 3.5$, respectively. It is observed that, FRF 1 can obtain the maximum cellular link capacity in both cases of $\alpha = 2.5$ and $\alpha = 3.5$. Therefore, the SC-FDAAA receiver can improve the bandwidth efficiency by using single frequency reuse.

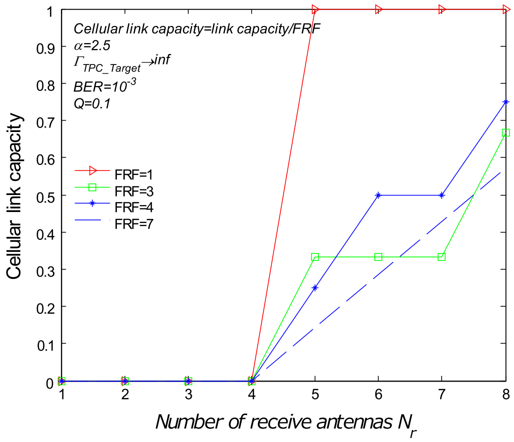

Fig. 11. Cellular link capacity, $\alpha = 2.5$.

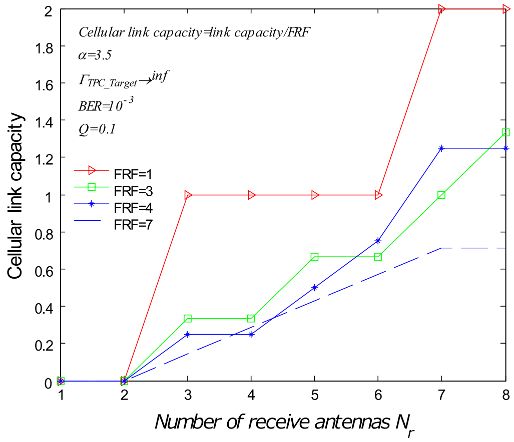

Fig. 12. Cellular link capacity, $\alpha = 3.5$.

On the other hand, it is noticed that, the cellular link capacity for $N_r = 8$ is 1 for $\alpha = 2.5$ and 2 for $\alpha = 3.5$ respectively, which can be further improved by using more advanced cellular structure. And this remains a topic of our future work.

6. Conclusions

In this paper, uplink multi-user MIMO transmission using SC-FDAAA in a cellular system has been studied. In order to make a comparison, two other weight control schemes, namely, SC-DC and SC-LS, have been introduced. Comparison between the SC-FDAAA and SC-DC and SC-LS schemes have been made in terms of computational complexity and BER performance. It has been shown that, the SC-FDAAA scheme has similar complexity as the SC-LS, while the performance of SC-FDAAA is the best among the three schemes. In addition, it has been shown that, the performance of the multi-user MIMO transmission can be realized. The BER performance and the capacity performance are affected by the number of receive antennas at the BS, the number of active users, the cellular structure as well as the path loss exponent. For FRF $=$ 1 case, two users/cell can be accommodated by a BS with 8 antennas; For FRF $>$ 1 case, 5 users/cell can be accommodated by a BS with 7 antennas. When cellular link capacity is considered, FRF 1 can obtain the best performance.

References

[1] G.J. Foschini, M.J. Gans, On limits of wireless communication in a fading environment when using multiple antennas, Wireless Personal Communications 6 (1998) 311–335.
[2] P.W. Wolniansky, G.J. Foschini, G.D. Golden, R.A. Valenzuela, V-BLAST: an architecture for realizing very high data rates over the rich-scattering wireless channel, in: URSI International Symposium on Signals, Systems, and Electronics, September 1998, pp. 295–300.
[3] J.H. Winters, J. Salz, R.D. Gitlin, The impacts of antenna diversity on the capacity of wireless communication systems, IEEE Transactions on Communications 42 (1994) 1740–1751.
[4] R. Kohno, Spatial and temporal communication theory using adaptive antenna array, IEEE Personal Communications 5 (1) (1998) 28–35.
[5] J.G. Proakis, Digital Communications, fourth ed., McGraw Hill, New York, 2001.
[6] R. Van Nee, R. Prasad, OFDM for Wireless Multimedia Communications, Artech House Publishers, UK, 1999.
[7] D. Falconer, S.L. Ariyavistakul, A. Benyamin-Seeyar, B. Edison, Frequency domain equalization for single-carrier broadband wireless systems, IEEE Communications Magazine 40 (2002) 58–66.
[8] G.L. Stuber, Principles of Mobile Communication, Kluwer Academic Publishers, Boston, 2000.
[9] M. Daoud Yacoub, Fading distributions and co-channel interference in wireless systems, IEEE Antennas and Propagation Magazine 42 (1) (2000) 150–160.
[10] W. Peng, F. Adachi, Frequency domain adaptive antenna array algorithm for single-carrier uplink transmission, in: Proc. IEEE PIMRC 2009, Tokyo, September 2009, pp. 1–5.
[11] S. Hara, R. Prasad, Overview of multicarrier CDMA, IEEE Communications Magazine 35 (1998) 126–133.
[12] B.W. Kang, K. Takeda, F. Adachi, Performance of single-carrier frequency-domain adaptive antenna array, in: IEEE Conference VTC Fall 2007, September 2007, pp. 491–495.
[13] Simon Haykin, Adaptive Filter Theory, Prentice Hall, New York, 2002.
[14] J.H. Winters, Signal acquisition and tracking with adaptive arrays in the digital mobile radio system IS-54 with flat fading, IEEE Transactions on Vehicular Technology 42 (1993) 377–384.
[15] M.A. Woodbury, Inverting Modified Matrices, Princeton, New Jersey, 1950.
[16] H.V. Henderson, S.R. Searle, On deriving the inverse of a sum of matrices, SIAM Review 23 (1) (1981) 53–60.
[17] F. Adachi, H. Tomeba, K. Takeda, Frequency-domain equalization for broadband single-carrier multiple access, IEICE-Transactions on Communications E92-B (5) (2009) 1441–1456.

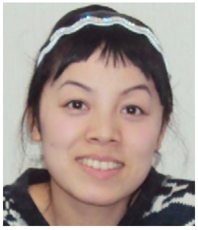

Wei Peng received her B.S. and M.S. degree in electrical engineering from Wuhan University, Wuhan, China, in 2000 and 2003 respectively. She received the Dr. Eng degree in electrical and electronic engineering from the University of Hong Kong in 2007. She jointed Tohoku University, Sendai, Japan, in 2007 and served as an assistant professor in the department of communication engineering. Since 2013, she joined Huazhong University of Science and Technology, Wuhan, China, and is currently an associate professor. Her research interests are in multiple antenna technology, single carrier transmission, distributed antenna network and etc.

Fumiyuki Adachi received the B.S. and Dr. Eng. degrees in electrical engineering from Tohoku University, Sendai, Japan, in 1973 and 1984, respectively. In April 1973, he joined the Electrical Communications Laboratories of Nippon Telegraph and Telephone Corporation (now NTT) and conducted various types of research related to digital cellular mobile communications. From July 1992 to December 1999, he was with NTT Mobile Communications Network, Inc. (now NTT DoCoMo,Inc.), where he led a research group on wideband/broadband CDMA wireless access for IMT-2000 and beyond. Since January 2000, he has been with Tohoku University, Sendai, Japan, where he is a Professor of Electrical and Communication Engineering at the Graduate School of Engineering. His research interests are in CDMA wireless access techniques, equalization, transmit/receive antenna diversity, MIMO, adaptive transmission, and channel coding, with particular application to broadband wireless communications systems.